Research Square

Preprints are preliminary reports that have not undergone peer review.
They should not be considered conclusive, used to inform clinical practice,
or referenced by the media as validated information.

Molecular characterisation of an Italian cohort of Silver-Russell Syndrome patients by -omics approaches

Flavia Cerrato
flavia.cerrato@unicampania.it

Università degli Studi della Campania “Luigi Vanvitelli” https://orcid.org/0000-0003-3794-3021
Emilia D’Angelo
Laura Pignata
Abu Saadat
Francesco Cecere
Aurora Esposito
Federica Rossetti
Carlo Giaccari
Angela Pagano
Carmelo Piscopo
Medical and Laboratory Genetics Unit, A.O.R.N. ‘Antonio Cardarelli’, Napoli, Italy
Maria Piccione
Elena Andreucci
Meyer Children's University Hopital https://orcid.org/0000-0002-4639-8144
Angela Sparago
University of Campania Luigi Vanvitelli https://orcid.org/0000-0003-4352-945X
Andrea Riccio
Second University of Naples https://orcid.org/0000-0001-7990-3576

Article

Keywords: Silver-Russell syndrome, imprinting disorders, growth retardation, DNA methylation, whole-exome sequencing

Posted Date: August 6th, 2026

DOI: https://doi.org/10.21203/rs.3.rs-10489286/v1

License: This work is licensed under a Creative Commons Attribution 4.0 International License. Read Full License

Additional Declarations: There is no duality of interest

Abstract

Silver-Russell syndrome (SRS) is an imprinting disorder primarily associated with growth retardation. A molecular diagnosis is achieved in about 60% of patients. The most common defect is loss of methylation (LoM) at the *H19/IGF2* imprinting locus on chromosome (chr) 11p15.5, followed by maternal uniparental disomy of chromosome 7 (upd(7)mat). Less frequent causes include single-nucleotide variants and copy-number variants in several other chromosome regions. About 40% of cases remain undiagnosed.

We investigated 61 Italian patients fulfilling the Netchine-Harbinson clinical scoring system (NH-CSS) criteria. Multi-locus DNA methylation analysis identified molecular alterations in 29 patients, including 24 with LoM at the *H19/IGF2* imprinted locus, 3 with upd(7)mat, 1 case with methylation abnormalities affecting chr14, and 1 case with an extremely rare maternal duplication involving the telomeric domain of chr11p15.5. Whole-exome sequencing (WES) of 32 molecularly negative patients identified pathogenic/likely pathogenic variants in genes associated with growth retardation in 12 cases. Two of these genes were absent from conventional gene panels. Genome-wide methylation analysis was performed in 48 SRS cases. We observed differentially methylated probes in promoter regions of genes implicated in growth, craniofacial, and skeletal development, supporting epigenetic deregulation extending beyond canonical imprinted loci.

Our findings highlight the molecular heterogeneity of SRS and support integrated diagnostic approaches. Alterations outside chr11 and chr7 represent the second most frequent molecular defect in our cohort. Genome-wide methylation profiling may also help identify genes involved in somatic growth across SRS molecular subgroups. Overall, these results support redefining SRS as a molecular rather than clinical diagnosis.

INTRODUCTION

Imprinting disorders (IDs) are a group of congenital diseases caused by genetic or epigenetic alterations affecting imprinted genes, a unique class of genes expressed monoallelically according to their parental origin [1]. Their expression is regulated by Imprinting Control Regions (ICRs, also known as Imprinting Centres, ICs), which contain differentially methylated regions (DMRs) established during gametogenesis and maintained throughout development. Disruption of these epigenetic marks results in abnormal expression of imprinted genes, leading to disturbances in fetal and postnatal growth, metabolism, neurodevelopment, and tumour susceptibility [1]. Because IDs are characterised by marked molecular heterogeneity and overlapping clinical phenotypes, molecular diagnosis remains challenging.

Among the thirteen recognised IDs, Silver-Russell syndrome (SRS; OMIM #180860) is one of the most molecularly heterogeneous. Clinically, SRS is characterised by intrauterine and postnatal growth restriction, relative macrocephaly at birth, protruding forehead, body asymmetry, and feeding difficulties. According to the NH-CSS, a clinical diagnosis is established when at least four of six core criteria are present [2]. However, the phenotype overlaps substantially with other growth restriction syndromes, and approximately 40% of clinically diagnosed patients remain without an identifiable molecular cause [2].

The most common molecular defects involve imprinted loci on chr 11p15.5 and 7. LoM at the *H19/IGF2*:IG-DMR (IC1) accounts for 30–60% of cases, while upd(7)mat is identified in 5–10%. Approximately 10–20% of patients with IC1 LoM also exhibit multilocus imprinting disturbances (MLID) [3]. Less frequent causes include maternal duplications of IC1, upd(11)mat, and pathogenic variants in imprinted genes such as *CDKN1C* and *IGF2*, as well as in upstream regulators of the *IGF2* pathway, including *PLAG1* and *HMGA2* [4–7].

Current diagnostic algorithms rely primarily on multi-locus methylation-specific multiplex ligation-dependent probe amplification (MS-MLPA), which detects abnormalities at chrs 11p15, 7, and additional imprinted loci associated with SRS-like phenotypes, including chrs 14q32, upd(16)mat, and upd(20)mat [2]. More recently, next-generation sequencing (NGS), including whole-exome sequencing (WES), has identified pathogenic variants in non-imprinted genes, demonstrating that many SRS-like cases represent distinct monogenic disorders [8–12]. Genome-wide methylation studies have also been explored but have not identified a consistent SRS-specific episignature, and reported findings remain inconsistent across studies.

Despite these advances, a substantial proportion of patients still lack a molecular diagnosis. Differences in sequencing strategies, bioinformatic pipelines, cohort composition, and methylation analysis methods have limited diagnostic yield and hindered cross-study comparisons.

Here, we present a comprehensive molecular investigation of 61 Italian patients with clinically diagnosed SRS (NH-CSS ≥ 4). We applied a tiered diagnostic strategy combining multi-locus MS-MLPA, WES with an extended bioinformatic pipeline in MS-MLPA-negative cases, and genome-wide DNA methylation profiling to improve diagnostic yield and evaluate the utility of epigenome-wide signatures for patient stratification.

SUBJECTS AND METHODS

Study cohort

The study cohort comprised 61 Italian patients (40 males, 21 females) who fulfilled the clinical criteria for SRS with NH-CSS ≥ 4. Detailed clinical features and individual diagnostic scores are provided in Supplementary Table S1.

DNA extraction

Genomic DNA of patients was isolated from peripheral blood leukocytes (PBLs) by the standard salting-out procedure [13]. DNA concentration was determined using the NanoDrop™ 2000c Spectrophotometer (Thermo Fisher Scientific).

DNA Methylation analyses

MS-MLPA was performed on PBL DNA from patients according to the manufacturer's instructions using the SALSA MS-MLPA Kit ME034-B1, ME034-C1, ME030 BWS/RSS (MRC-Holland, Amsterdam, The Netherlands).

Pyrosequencing analysis was performed as previously described [14].

Single Nucleotide Polymorphisms (SNP)-array

SNP-array was conducted using Illumina's Infinium Global Screening Array-24 v3.0 (GSAv3) (Illumina, San Diego, CA, USA), which interrogates approximately 650,000 markers, according to the manufacturer's instructions. Raw data were imported from iScan Control Software into Genome Studio 2.0 Software (Illumina).

Whole-exome sequencing

Library preparation, DNA enrichment and sequencing were performed as previously described [15]. WES data preprocessing followed the nf-core Sarek pipeline (version 3.3.2) using default settings. Sequencing reads were mapped to the human reference genome GRCh38 using the BWA-MEM algorithm. Variant identification was performed using DeepVariant [16]. A quality score threshold of 20 and a minimum read depth of 15 were applied as filters for variant selection.

The resulting variant call format (VCFs) files were processed with two different bioinformatics approaches. First, VCF files were annotated with the Variant Effect Predictor (VEP, version 111.0). Population frequency filters (MAF $\leqslant$ 0.01) were applied based on the gnomAD database. Annotated variants were intersected with gene panels to identify alterations in genes already linked to growth retardation [5, 8] (Supplementary Table S2). The second approach included a more extensive analysis to identify new candidate genes based on the predicted pathogenicity of the variants and specific clinical phenotypes of individual patients. In this latter case, VCF files were annotated and analysed using Franklin by Genoox.

In both approaches, in silico pathogenicity prediction was performed using CADD v1.7, PolyPhen-2, SIFT, AlphaMissense, REVEL, and SpliceAI. All variants were classified according to the ACMG (American College of Medical Genetics) standards and guidelines [17, 18]. For familial cases, WES was also performed on parental DNA when available.

Genome-wide DNA methylation analysis

Genome-wide DNA methylation was assessed in bisulfite-converted PBL DNA samples using the Illumina Infinium MethylationEPIC v2.0 BeadChip array (Biodiversa, Italy). Raw IDAT files were processed as previously reported [19, 20], as well as the methylation analysis of the imprinted DMRs and DMPs.

RESULTS

Methylation and CNV analysis of the clinical imprinted loci

Comprehensive molecular profiling was performed on a cohort of 61 Italian patients who met the clinical criteria for SRS with NH-CSS ≥ 4 (Fig. 1). All subjects initially underwent screening for CNV and methylation status at 11 imprinted loci using the multi-locus MS-MLPA assay. Molecular alterations were identified in 29 of 61 patients (47.5%; Supplementary Table S3).

Most of these cases (24/29) exhibited LoM at the IC1 locus on chr11p15.5. Within this subgroup, patient SRS1 presented with MLID, characterised by additional slight LoM at the *KCNQ1OT1*:TSS-DMR in the absence of detectable CNVs (previously described in Passaretti F. et al., 2022 [21]). In patient SRS25, multi-locus MLPA analysis first identified a microduplication encompassing the *H19* locus without evident methylation defect (Fig. 2A). Regarding chr7, three patients (SRS26–SRS28) displayed hypermethylation at both the *GRB10*:alt-TSS-DMR and *MEST*:alt-TSS-DMR, suggestive of an upd(7)mat. Finally, patient SRS29 showed a distinct chr14 profile, with hypomethylation at the *MEG3*:TSS-DMR and hypermethylation at the *MEG8*:Int2-DMR.

To further characterise the duplication in SRS25, we employed the MS-MLPA ME030 (BWS/SRS) assay, which includes a denser set of probes spanning the 11p15 imprinting cluster. The analysis confirmed a duplication of the *H19* gene associated with a slight LoM at the IC1 (Fig. 2A). The methylation defect was more clearly detected by bisulfite/pyrosequencing analysis of the CTCF target site 1 (CTS1) within the *H19/IGF2*:IG-DMR, probably because of the higher sensitivity of this technique (Fig. 2B and 2C; Supplementary Table S4). Combined MS-MLPA and pyrosequencing data demonstrated that the duplication encompasses the entire *H19/IGF2*:IG-DMR and the *H19* gene, but excludes *IGF2* (Fig. 2C). Due to limited DNA availability, the precise breakpoints of the duplication could not be mapped. Additionally, the lack of parental DNA precluded determination of whether the duplication arose *de novo* or via maternal transmission. Nonetheless, the observed hypomethylation at the IC1 region strongly suggests that the duplication selectively affected the maternal allele.

In summary, molecular etiologies were first identified in 29/61 (47.5%) of the cohort: 24 cases of IC1 LoM (including one MLID case), one rare *H19* duplication, three cases with chr7 methylation defects, and one case with chr14 alterations.

Genome-wide CNV and UPD detection

SNP-array analysis was used to characterise methylation defects at chr7 and chr14. Upd(7)mat was identified in all three patients exhibiting hypermethylation at both the *GRB10*:alt-TSS-DMR and *MEST*:alt-TSS-DMR loci (SRS26, SRS27, and SRS28). These cases displayed varying patterns of

isodisomy and heterodisomy (Supplementary Fig. 1, Supplementary Table S5). Specifically, patient SRS26 displayed a single isodisomic region in the long arm of chr7 (Supplementary Fig. 1A). The maternal origin of upd was confirmed through the analysis of the TRIO DNA (Supplementary Table S6). SRS27 exhibited a more complex profile with two isodisomic regions on chr7 and a mosaic 45XO/46XX karyotype (Supplementary Fig. 1B). This finding was consistent with a referred karyotyping that identified three-cell-line mosaicism (68% 46,XX; 25% 45,X with a chr7 marker; 7% 45,X). SRS28 featured an isodisomic segment spanning the centromere (Supplementary Fig. 1C). In contrast, the patient with chr14 methylation defects (SRS29) showed a normal SNP-array profile with no evidence of upd or chromosomal imbalance (Supplementary Fig. 1D).

These results confirmed that all cases of altered chr7 imprinting were caused by upd(7)mat. Conversely, the chr14 defect in SRS29 was associated with no detectable chromosomal abnormalities, suggesting a primary imprinting defect.

Identification of potentially causative gene variants

WES data were obtained from 32 patients who had previously tested negative by multi-locus MS-MLPA analysis (Fig. 1). Among these, three were familial cases, and TRIO analysis was performed for SRS43 and SRS44, while only maternal DNA was available for case SRS42. Comparison with literature-based gene panels revealed variants in *CUL7, PIK3R1, NF1, FANCA* and *HRAS.* Subsequent extensive exome analysis revealed additional variants in *NSD2* and *KMT2D*, two genes not included in the primary panels (Table 1, Supplementary Table S7).

Table 1
List of the putative pathogenic or likely pathogenic variants identified in 12 patients of our cohort by WES.

Patient	Gene	Genomic DNA level (hg38)	Coding level	Protein level	Effect	Variant ID (dbSNP)	Zygosity	Inheritance	gnomAD Exomes frequency
SRS30	*CUL7*	chr6:43038891 T > G	NM_014780.5: c.4391A > C	p.His1464Pro	missense	rs121918229	het	paternal	0.0000131
	CUL7	chr6:43046026 C > T	NM_014780.5: c.2726G > A	p.Gly909Glu	missense	rs769343287	het	maternal	0.0000065
SRS31	*CUL7*	chr6:43038891 T > G	NM_014780.5: c.4391A > C	p.His1464Pro	missense	rs121918229	hom	paternal/ maternal	0.0000131
SRS32	*PIK3R1*	chr5:68296301 C > T	NM_181523.3: c.1945C > T	p.Arg649Trp	missense	rs397515453	het	de novo	not found
SRS33	*PIK3R1*	chr5:68296301 C > T	NM_181523.3: c.1945C > T	p.Arg649Trp	missense	rs397515453	het	NA	not found
SRS34	*NF1*	chr17:31229356 G > A	NM_001042492.3: c.2741G > A	p.Arg914Gln	missense	rs776447057	het	NA	0.0000065
SRS35	*NF1*	chr17:31229356 G > A	NM_001042492.3: c.2741G > A	p.Arg914Gln	missense	rs776447057	het	NA	0.0000065
SRS36	*NF1*	chr17:31203089 A > G	NM_001042492.3: c.1260 + 1604A > G	p.?	intronic (splice mutation)	rs1131691067	het	NA	not found
SRS37	*FANCA*	chr16:89803261 G > A	NM_000135.4: c.790C > T	p.Gln264*	stop gain	rs1353992080	het	NA	0.0000013
	FANCA	chr16:89739290 CTA > C	NM_000135.4: c.4011-3_4011-2del	p.?	intronic (splice mutation)	rs911481295	het	NA	0.0000013
SRS38	*HRAS*	chr11:534255 A > C	NM_005343.4: c.68T > G	p.Leu23Arg	missense	-	het	NA	-
SRS39	*NSD2*	chr4:1953463 C > A	NM_001042424.3: c.2277C > A	p.Cys759*	stop gain	-	het	NA	-
SRS40	*NSD2*	chr4:1935242 GA > G	NM_001042424.3: c.1655del	p.Asp552Alafs*46	frameshift (premature stop)	-	het	de novo	-

het: heterozygous; hom: homozygous; NA: not analysed; AR: Autosomal Recessive; AD: Autosomal Dominant.

Patient	Gene	Genomic DNA level (hg38)	Coding level	Protein level	Effect	Variant ID (dbSNP)	Zygosity	Inheritance	gnomAD Exomes frequency
SRS41	*KMT2D*	chr12:49026509 G > A	NM_003482.4: c.15457C > T	p.Arg5153Trp	missense	rs761700549	het	NA	0.0000006

het: heterozygous; hom: homozygous; NA: not analysed; AR: Autosomal Recessive; AD: Autosomal Dominant.

Patients SRS30 and SRS31 showed a likely pathogenic variant in *CUL7* (p.His1464Pro). In SRS30, the variant was detected in compound heterozygosity with a rare, predicted-deleterious, missense mutation (p.Gly909Glu). In SRS31, the p.His1464Pro variant was present in homozygosity, likely reflecting parental consanguinity. Interestingly, pathogenic variants in *CUL7* are a well-established cause of 3-M syndrome, a disorder with substantial clinical overlap with SRS [22]. Patients SRS32 and SRS33 both carried the same heterozygous pathogenic variant in *PIK3R1* (p.Arg649Trp). In SRS32, Sanger sequencing of the TRIO confirmed the variant was *de novo*, whereas parental samples were unavailable for SRS33. The p.Arg649Trp variant has previously been reported in multiple individuals with SHORT syndrome [23].

Likely pathogenic variants in *NF1*, causative of Neurofibromatosis-Noonan syndrome [5], were identified in three individuals. Monozygotic twins (SRS34 and SRS35) shared a rare heterozygous missense variant (p.Arg914Gln) and presented with *cafè au lait* spots, consistent with the *NF1* phenotype [11]. Patient SRS36 carried a heterozygous intronic variant (chr17-31203089 A > G) predicted to disrupt splicing. Patient SRS37 harboured two pathogenic heterozygous variants in *FANCA*: a stop gain variant (p.Gln264*) and a splice region variant (chr16-89739290 CTA > C). While compound heterozygosity is suspected, it could not be confirmed without parental DNA. *FANCA* variants have been previously documented in patients presenting with SRS features [11].

Patient SRS38 presented with a novel missense variant in *HRAS* (p.Leu23Arg), related to Noonan syndrome [5], a disorder characterised by growth disturbances and variable neuro-cardio-facio-cutaneous features. Interestingly, the patient was referred to show *cutis marmorata*, a reticulated cutaneous vascular pattern with altered colour (red or blue), which is a tegumentary alteration associated with Noonan and Noonan-related syndromes [24]. Variants in chromatin remodeling genes were identified in three patients. SRS39 and SRS40 carried heterozygous variants in *NSD2*: a stop-gain variant (p.Cys759*) and a *de novo* frameshift deletion (p.Asp552Alafs*46), respectively, leading to premature termination codons. Finally, SRS41 harboured a rare missense variant in *KMT2D* (p.Arg5153Trp), typically associated with Kabuki syndrome (KS), whose clinical features include primarily prenatal and postnatal growth restriction.

Overall, pathogenic/likely pathogenic variants potentially accounting for the growth retardation phenotype were identified in 10 cases plus a twin pair (11/31, 35.5%). A detailed analysis of WES data revealed putative causative variants in two genes, *NSD2* and *KMT2D*, which are not included in commonly used panels.

WES was also performed on two mothers of SRS cases with upd(7)mat (SRS26, SRS27). Interestingly, both cases carried a heterozygous variant in the *RECQL4* gene. The mother of SRS27 carried a rare pathogenic stop-gain mutation (p.Arg758*), affecting the helicase domain, while the mother of SRS26 carried a rare missense variant with uncertain pathogenicity (VUS; p. Val910Ile).

Genome-wide methylation analysis

We determined genome-wide methylation profiles with the Illumina MethylationEPIC array. This analysis was carried out in 48 SRS cases with or without previously identified molecular defects and 20 healthy individuals (Supplementary Table S1). First, we examined methylation levels at imprinted regions, extending the analysis beyond the imprinted DMRs previously tested by multi-locus MS-MLPA. By applying the criteria described in Cecere&Pignata and Cecere et al. (2025)[19, 20], we found no additional cases with MLID (Supplementary Table S8). We then focused on the genome-wide identification of Differentially Methylated Probes (DMPs), defined as CpGs showing a mean methylation difference of at least 10% and an adjusted p-value < 0.05. We compared the SRS patients' group against controls and identified 11823 DMPs. We next focused the analysis on sites within promoter regions (Supplementary Table S9) and selected genes that carried at least 3 promoter-associated differentially methylated CpGs (Supplementary Table S10). Notably, *HOXA4* had the highest number of promoter-associated DMPs, with 14 sites identified (Supplementary Table S10). This gene belongs to the cluster of *HOXA* genes located on chr7p15.2 and may play a role in growth-regulating pathways. Given the enrichment of DMPs on *HOXA4*, we extended the analysis to the entire locus and observed that the entire promoter region was hypomethylated (Fig. 3A; Supplementary Table S11). To determine whether *HOXA4* promoter hypomethylation was mainly associated with a specific SRS molecular subgroup, we stratified patients into three groups: cases with IC1 LoM, cases with identified causative genetic variants and cases without an identified molecular cause. Mean methylation levels at individual CpG sites did not differ among the three SRS groups, indicating a consistent epigenetic profile (Fig. 3A; Supplementary Table S11). We next analysed patient-specific methylation patterns, defining hypomethylation for an individual when at least two-thirds of the 14 *HOXA4* DMPs showed values below − 2SD of the control mean. Overall, 52% of patients were classified as hypomethylated (11/20 IC1 LoM, 7/11 SRS with genetic variants and 7/17 idiopathic SRS) (Supplementary Table S12).

LTBP1 was the second gene with the highest number of DMPs in both groups (Supplementary Table S10). The protein encoded by this gene belongs to the family of latent TGF-beta binding proteins (LTBPs). *LTBP1* encodes two alternatively spliced isoforms: a long (*LTBP1L*) and a short (*LTBP1S*) isoform. The promoter and transcription start site for *LTBP1S* lie within the 4th intron of *LTBP1L*. The DMPs identified in our cohort showed increased methylation levels compared with healthy controls (Fig. 3B, Supplementary Table S13). Stratification of the patients showed that this hypermethylation pattern was present in all three molecular subgroups (Fig. 3B, Supplementary Table S13). Patients were classified as hypermethylated when at least two-thirds of the DMPs exceeded +2SD of the control mean. Based on this threshold, we identified a methylation defect in 31% of cases (7/20 IC1 LoM, 4/11 SRS with genetic variants and 4/17 idiopathic SRS) (Supplementary Table S14). Notably, in our cases, the DMPs were mapped to the promoter region of *LTBP1S* (Fig. 3C).

To further explore the list of genes with promoter-associated DMPs, we assessed the enrichment of human phenotypes using the Human Phenotype Ontology (HPO) and OMIM annotations. We focused on three pre-specified axes of interest: i) short stature/growth delay (HPO:0004322 and descendants); ii) abnormality of the face/ craniofacial morphology (HPO: 0000271 and descendants); iii) abnormality of the skeletal system (HPO: 0000924 and descendants). OMIM entries and literature references were used to contextualise the most relevant associations. We identified several candidates associated with the selected phenotypes. In particular, we confirmed *HOXA4* and *LTBP1* as key candidates, with additional associations involving *HOXA2, SPRED2, EDARADD* and *ELN*, supporting their roles in growth, craniofacial and skeletal traits (Supplementary Fig. 2, Supplementary Table S15).

In summary, genome-wide methylation analysis revealed methylation changes on the promoter region of genes involved in the regulation of growth, craniofacial morphology and skeletal development in the patients regardless of their molecular subgroup.

DISCUSSION

This study provides a comprehensive molecular characterisation of a well-defined Italian cohort of 61 patients fulfilling the clinical criteria for SRS, using a tiered diagnostic strategy integrating multi-locus MS-MLPA, WES, and genome-wide methylation profiling. This approach achieved a molecular diagnosis in 67% of clinically diagnosed patients and further highlighted the molecular and epigenetic heterogeneity underlying the SRS phenotype.

Detection of methylation defects at imprinted loci

Multi-locus MS-MLPA, used as first-tier screening, identified a molecular defect in 47.5% (29/61) of the cohort, consistent with previously reported rates in comparable populations [2, 3]. LoM at *H19/IGF2*:IG-DMR was, as expected, the most frequent finding, accounting for ~ 39% (24/61) of cases. MLID was exceptionally rare, found in only one patient (SRS1), who also showed hypomethylation at *KCNQ1OT1*:TSS-DMR. Detection of upd(7)mat in three patients (4.9%) and a primary chr14 imprinting defect in one further patient are consistent with the known SRS molecular spectrum and confirm the utility of multi-locus panels for imprinted-locus alterations.

Our screening also identified a rare maternal chr11p15.5 microduplication in patient SRS25. Maternal 11p15.5 duplications occur in < 1% of SRS patients [25], and those limited to the telomeric domain are very rare. Maternal duplications of the entire telomeric domain (including *H19* and *IGF2*) do not cause growth restriction [26], whereas duplications involving *H19* and IC1 but excluding *IGF2* have been reported in three SRS patients [27–29]. Both types yield two active maternal *H19* copies but likely differ in chromatin organisation. Beyond its cis-regulatory role, *H19* lncRNA can repress *Igf2* in trans: *H19* transgenic expression rescues overgrowth and reduces *Igf2* levels in *H19* knockout mice [30]. Thus, in partial telomeric duplications, an extra functional maternal *H19* copy may suppress *IGF2* via a trans-acting mechanism, driving the growth restriction observed in SRS25 [29]

Combined MS-MLPA and SNP-array confirmed upd(7)mat in all three patients, showing hypermethylation of both *GRB10* and *MEST*. The presence of mixed heterodisomy and isodisomy supports a mechanism involving maternal meiotic nondisjunction followed by trisomy rescue. One patient (SRS27) also displayed a mosaic 45,XO/46,XX karyotype, indicating an additional postzygotic chromosome segregation error. Interestingly, the mothers of two upd(7)mat patients carried rare *RECQL4* variants, one pathogenic and one classified as a variant of uncertain significance, and both had histories of recurrent miscarriage. Although upd(7)mat is generally considered sporadic, these findings raise the possibility that maternal *RECQL4* variants may predispose to chromosome segregation errors during oogenesis or early embryogenesis, a hypothesis warranting further investigation.

Regarding phenotype, skeletal asymmetry was more frequent in the IC1 LoM group than in upd(7)mat cases (73.9% vs. 33.3%), confirming previous findings [2, 31]. Downturned mouth corners (78.3% vs. 0%), thin upper lip (87% vs. 33.3%), and brachydactyly/clinodactyly V (87% vs. 33.3%) clustered preferentially in IC1 LoM, whereas upd(7)mat showed higher prevalence of oligohydramnios (100% vs. 30.4%), postnatal growth restriction (100% vs. 69.6%), and retarded bone age (66.7% vs. 4.3%), underscoring upd(7)mat's severe impact on growth and gestational development (Supplementary Table S1).

Patient SRS29 presented with an isolated chr14 imprinting defect (*MEG3*:TSS-DMR hypomethylation, *MEG8*:Int2-DMR hypermethylation) on a normal SNP-array background. Although chr14q32 alterations typically define Temple syndrome, > 8% of SRS patients with NH-CSS ≥ 4 harbour similar alterations [32], reflecting the broader clinical and epigenetic overlap between these growth-restriction disorders and the limitations of phenotype-based diagnostic criteria. Consistently, SRS29 displayed features of both conditions: hypotonia and neurodevelopmental delay suggestive of Temple syndrome, alongside skeletal asymmetry, prominent forehead, and relative macrocephaly typical of SRS.

WES reveals molecular diagnoses beyond classical imprinting defects

Among the 32 patients negative for canonical imprinting defects, WES identified pathogenic/likely pathogenic variants in 35.5% (11/31; twins counted once), a diagnostic expansion supporting the emerging view that many "idiopathic" SRS cases represent distinct monogenic phenocopies driven by mutations in non-imprinted growth pathways [9, 10]. Variants were mapped in seven genes. *CUL7* variants, confirmed in two patients as the basis of 3-M syndrome, represent perhaps the most clinically pertinent overlap given the phenotypic similarity between 3-M syndrome and SRS [2, 33], reinforcing recommendations to include *CUL7* screening in NH-CSS-positive, imprinting-negative patients. Similarly, *PIK3R1* p.Arg649Trp in two patients confirms SHORT syndrome as a recurrent SRS mimic [8, 12]; its *de novo* occurrence in SRS32 underscores the diagnostic value of TRIO sequencing in apparent simplex cases. *NF1* variants were identified in three patients, including monozygotic twins. Neurofibromatosis type 1 and Noonan syndrome with multiple lentigines produce RASopathy-related growth restriction that can fulfil NH-CSS criteria, particularly when *café-au-lait* spots are subtle [11, 34]; *cutis marmorata* in the *HRAS*-variant patient (SRS38) provided an informative clue, as vascular tegumentary changes are recognised in Noonan-related disorders [24]. These cases highlight the importance of comprehensive clinical re-evaluation, including dermatological assessment, before attributing growth restriction to SRS. A *FANCA* variant identified in one patient further extends SRS genetic heterogeneity, consistent with documented overlap between Fanconi anemia and SRS regarding growth restriction and mild dysmorphism [11].

An extended bioinformatic workflow beyond standard growth-restriction panels also identified pathogenic variants in two major chromatin remodelling genes, *NSD2* and *KMT2D. NSD2* loss-of-function variants cause Wolf–Hirschhorn-like phenotypes and have been proposed as a critical SRS differential diagnosis [35], while *KMT2D*, classically linked to Kabuki syndrome, shows documented overlapping presentations. These findings highlight the limitations of panel-based WES when panels are not continuously updated with emerging gene-disease associations, supporting phenotype-driven exome analysis as a complementary or primary strategy in diagnostically challenging cases.

Overall, our WES results corroborate growing evidence that a substantial fraction of patients fulfilling NH-CSS criteria harbour molecular diagnoses distinct from classical SRS, indicating that the NH-CSS functions as a broad clinical gateway for a heterogeneous phenotype rather than a molecularly homogeneous condition [9, 10, 12]. While WES lacks the capacity of genome sequencing to detect non-coding or complex structural variants, our diagnostic yield was comparable to recent genome sequencing cohorts [9]; the apparent difference (35.5% vs 50%) likely reflects our more stringent inclusion criteria (NH-CSS ≥ 4, exclusion of VUS). This comparable efficiency likely reflects that pathogenic SNVs identified so far in monogenic differential diagnoses reside within coding regions equally covered by both platforms.

Shared epigenomic perturbations across SRS molecular subgroups

Genome-wide methylation analysis using the Illumina MethylationEPIC v2.0 array in 48 patients and 20 controls provided insights into the SRS epigenomic landscape. Consistent with prior studies using similar platforms [36–39], no single SRS-specific episignature was identified. The most striking finding was a shared, overlapping network of differentially methylated positions across the promoter regions of *HOXA4* and *LTBP1* in all SRS molecular subgroups, suggesting shared epigenetic alterations in growth and skeletal development pathways irrespective of the underlying molecular defect. Hypomethylation of the *HOXA4* promoter, observed in 52% of patients, suggests a role for this gene in growth-control processes; *HOXA4*, a member of the *HOXA* cluster on chr7p15.2, encodes a transcription factor essential for gene expression regulation, morphogenesis, and differentiation, and prior studies have proposed abnormal *HOXA4* methylation as contributing to SRS skeletal defects [40]. Notably, Kabuki syndrome patients show global DNA methylation abnormalities including hypomethylation near this gene [41], and 3-M syndrome is characterised by *IGF2* downregulation with *HOX* gene upregulation [42], supporting interaction between *HOX*-dependent networks and *IGF2* signalling in modulating postnatal growth.

Hypermethylation of the *LTBP1* promoter in ~ 31% of patients is similarly notable. *LTBP1* encodes an extracellular matrix component regulating bioavailability and activation of latent TGF-β, a central pathway governing embryonic growth, skeletal development, and craniofacial morphogenesis [43]. The *LTBP1S* isoform, whose transcription start site was hypermethylated in our cohort, shows distinct expression patterns and functional roles compared to *LTBP1L*; promoter hypermethylation would be predicted to reduce *LTBP1S* expression, with downstream consequences for TGF-β signalling plausibly contributing to growth restriction and skeletal abnormalities.

Broader enrichment analysis using HPO and OMIM annotations identified additional candidate genes with established roles in growth, craniofacial morphology, and skeletal biology [44, 45]. The convergence of epigenomic perturbations at growth- and craniofacial-pathway genes across molecularly distinct SRS cases supports the hypothesis that, regardless of primary molecular cause, SRS phenotypes may arise partly through shared downstream epigenomic dysregulation affecting overlapping developmental gene networks.

Conclusions

Our tiered diagnostic strategy resolved the molecular etiology in nearly two-thirds of this Italian SRS cohort. MS-MLPA identified an imprinting defect at a known SRS-associated locus in approximately half of the cohort, confirming this as the leading cause of the classical phenotype. WES combined with extensive bioinformatic analysis proved essential to characterise further 18% of NH-CSS-positive patients who carried molecular diagnoses distinct from canonical SRS imprinting defects.

Genome-wide methylation profiling further revealed that molecularly distinct SRS subgroups converge on shared epigenomic perturbations at developmentally relevant loci, most notably *HOXA4* and *LTBP1*. This convergence suggests that phenotypically overlapping growth-restriction disorders may act through common downstream epigenomic mechanisms to produce the shared SRS phenotype. Validation in larger, international cohorts will be needed to determine whether these promoter alterations can serve as auxiliary biomarkers to improve diagnostic stratification of patients with idiopathic growth restriction.

These findings highlight the substantial genetic and epigenetic heterogeneity underlying clinically diagnosed SRS and support a model in which distinct molecular lesions converge on shared developmental pathways. We therefore propose that SRS be regarded as a molecular diagnosis, defined by identification of the causative genetic or epigenetic defect, rather than by clinical criteria alone.

Declarations

Data availability

Data supporting the conclusions of this article are included within the article and its supplementary files. Additional datasets are available from the corresponding authors on reasonable request.

Acknowledgements

The authors sincerely thank the patients and their families for their participation in this research project.

Author Contributions

E.D'A. , Fl.C. and A.R. designed experiments and interpreted results. E.D'A., L.P., A.E., C.G., and A.P. performed experiments. An. S., Ab.S., Fr.C. and F.R. supervised bioinformatics analyses. C.P., M.P. and E.A. provided clinical cases. E.D'A., Fl.C. and A.R. wrote the manuscript with input from all authors. All authors reviewed the manuscript.

Funding

This work was supported by grants from the Fondazione Telethon (GMR23T1062) to A.R. and Regione Campania (MARADONA Project) to A.R., Fl.C. and An.S.

Ethical approval

The study was approved by the ethical committees of the University of Campania Luigi Vanvitelli (Naples, Italy; approval number: 10423, 5 May 2020). Written informed consent for genetic testing and data publication was obtained from all participants or their parents/legal guardians.

Competing interest

All authors declare that they have no conflicts of interest.

References

1. Eggermann T, Monk D, De Nanclares GP, Kagami M, Giabicani E, Riccio A, et al. Imprinting disorders. Nat Rev Dis Primers. 2023;9(1):33. doi:10.1038/s41572-023-00443-4
2. Wakeling EL, Brioude F, Lokulo-Sodipe O, O'Connell SM, Salem J, Bliek J, et al. Diagnosis and management of Silver–Russell syndrome: first international consensus statement. Nat Rev Endocrinol. 2017;13(2):105–24. doi:10.1038/nrendo.2016.138
3. Mackay DJG, Gazdagh G, Monk D, Brioude F, Giabicani E, Krzyzewska IM, et al. Multi-locus imprinting disturbance (MLID): interim joint statement for clinical and molecular diagnosis. Clin Epigenet. 2024;16(1):99. doi:10.1186/s13148-024-01713-y
4. Abi Habib W, Brioude F, Edouard T, Bennett JT, Lienhardt-Roussie A, Tixier F, et al. Genetic disruption of the oncogenic HMGA2–PLAG1–IGF2 pathway causes fetal growth restriction. Genetics in Medicine. 2018;20(2):250–8. doi:10.1038/gim.2017.105
5. Alhendi ASN, Lim D, McKee S, McEntagart M, Tatton-Brown K, Temple IK, et al. Whole-genome analysis as a diagnostic tool for patients referred for diagnosis of Silver-Russell syndrome: a real-world study. J Med Genet. 2022;59(6):613–22. doi:10.1136/jmedgenet-2021-107699
6. Brioude F, Netchine I, Praz F, Le Jule M, Calmel C, Lacombe D, et al. Mutations of the Imprinted *CDKN1C* Gene as a Cause of the Overgrowth Beckwith-Wiedemann Syndrome: Clinical Spectrum and Functional Characterization. Human Mutation. 2015;36(9):894–902. doi:10.1002/humu.22824
7. D'Angelo E, Pignata L, Cecere F, Vimercati A, Cubellis MV, Saadat A, et al. Hypomethylation of the MEG8:Int2-DMR in patients with pathogenic PLAG1 variants suggests new role of the chr14q32 imprinting cluster in Silver-Russell syndrome. Clin Epigenetics. 2025;18(1):2. doi:10.1186/s13148-025-02024-6 PubMed PMID: 41276848; PubMed Central PMCID: PMC12764072.
8. Inoue T, Nakamura A, Iwahashi-Odano M, Tanase-Nakao K, Matsubara K, Nishioka J, et al. Contribution of gene mutations to Silver-Russell syndrome phenotype: multigene sequencing analysis in 92 etiology-unknown patients. Clin Epigenet. 2020;12(1):86. doi:10.1186/s13148-020-00865-x
9. Kessler L, Krause J, Kraft F, Amin AK, Fekete G, Lengyel A, et al. Diagnostic Use of Genome Sequencing in Patients With 11p15.5 Imprinting Disorder Features: A Pilot Study. Clinical Genetics. 2025;107(3):278–91. doi:10.1111/cge.14649
10. Meyer R, Soellner L, Begemann M, Dicks S, Fekete G, Rahner N, et al. Targeted Next Generation Sequencing Approach in Patients Referred for Silver-Russell Syndrome Testing Increases the Mutation Detection Rate and Provides Decisive Information for Clinical Management. The Journal of Pediatrics. 2017;187:206–212.e1. doi:10.1016/j.jpeds.2017.04.018
11. Meyer R, Begemann M, Hübner CT, Dey D, Kuechler A, Elgizouli M, et al. One test for all: whole exome sequencing significantly improves the diagnostic yield in growth retarded patients referred for molecular testing for Silver–Russell syndrome. Orphanet J Rare Dis. 2021;16(1):42. doi:10.1186/s13023-021-01683-x
12. Vimercati A, Tannorella P, Guzzetti S, Calzari L, Gentilini D, Manfredini E, et al. Distinguishing Genetic Alterations Versus (Epi)Mutations in Silver–Russell Syndrome and Focus on the *IGF1R* Gene. The Journal of Clinical Endocrinology & Metabolism. 2025;110(4):e932–44. doi:10.1210/clinem/dgae730
13. Miller SA, Dykes DD, Polesky HF. A simple salting out procedure for extracting DNA from human nucleated cells. Nucl Acids Res. 1988;16(3):1215–1215. doi:10.1093/nar/16.3.1215
14. Pignata L, Palumbo O, Cerrato F, Acurzio B, De Álava E, Roma J, et al. Both Epimutations and Chromosome Aberrations Affect Multiple Imprinted Loci in Aggressive Wilms Tumors. Cancers. 2020;12(11):3411. doi:10.3390/cancers12113411
15. Pignata L, Cecere F, Verma A, Hay Mele B, Monticelli M, Acurzio B, et al. Novel genetic variants of KHDC3L and other members of the subcortical maternal complex associated with Beckwith–Wiedemann syndrome or Pseudohypoparathyroidism 1B and multi-locus imprinting disturbances. Clin Epigenet. 2022;14(1):71. doi:10.1186/s13148-022-01292-w
16. Poplin R, Chang PC, Alexander D, Schwartz S, Colthurst T, Ku A, et al. A universal SNP and small-indel variant caller using deep neural networks. Nat Biotechnol. 2018;36(10):983–7. doi:10.1038/nbt.4235
17. Richards S, Aziz N, Bale S, Bick D, Das S, Gastier-Foster J, et al. Standards and guidelines for the interpretation of sequence variants: a joint consensus recommendation of the American College of Medical Genetics and Genomics and the Association for Molecular Pathology. Genetics in Medicine. 2015;17(5):405–24. doi:10.1038/gim.2015.30

18. Riggs ER, Andersen EF, Cherry AM, Kantarci S, Kearney H, Patel A, et al. Technical standards for the interpretation and reporting of constitutional copy-number variants: a joint consensus recommendation of the American College of Medical Genetics and Genomics (ACMG) and the Clinical Genome Resource (ClinGen). Genetics in Medicine. 2020;22(2):245–57. doi:10.1038/s41436-019-0686-8
19. Cecere F, Relator R, Levy M, Verma A, McConkey H, Mele BH, et al. Identification of genetic and non-genetic modifiers of genomic imprinting through screening of imprinted DMR methylation in humans. Epigenetics & Chromatin. 2025;18(1):47. doi:10.1186/s13072-025-00612-7
20. Cecere F, Pignata L, D'Angelo E, Giaccari C, Saadat A, Sparago A, et al. Highly variable genomic methylation in the Beckwith-Wiedemann syndrome associated with multi-locus imprinting disturbances. Clin Epigenet. 2025;17(1):160. doi:10.1186/s13148-025-01971-4
21. Passaretti F, Pignata L, Vitiello G, Alesi V, D'Elia G, Cecere F, et al. Different Mechanisms Cause Hypomethylation of Both H19 and KCNQ1OT1 Imprinted Differentially Methylated Regions in Two Cases of Silver-Russell Syndrome Spectrum. Genes (Basel). 2022;13(10):1875. doi:10.3390/genes13101875 PubMed PMID: 36292759; PubMed Central PMCID: PMC9602374.
22. Huber C, Dias-Santagata D, Glaser A, O'Sullivan J, Brauner R, Wu K, et al. Identification of mutations in CUL7 in 3-M syndrome. Nat Genet. 2005;37(10):1119–24. doi:10.1038/ng1628
23. Dyment DA, Smith AC, Alcantara D, Schwartzentruber JA, Basel-Vanagaite L, Curry CJ, et al. Mutations in PIK3R1 cause SHORT syndrome. Am J Hum Genet. 2013;93(1):158–66. doi:10.1016/j.ajhg.2013.06.005 PubMed PMID: 23810382; PubMed Central PMCID: PMC3710754.
24. Quaio CRDC, de Almeida TF, Brasil AS, Pereira AC, Jorge AAL, Malaquias AC, et al. Tegumentary manifestations of Noonan and Noonan-related syndromes. Clinics (Sao Paulo). 2013;68(8):1079–83. doi:10.6061/clinics/2013(08)03 PubMed PMID: 24037001; PubMed Central PMCID: PMC3752636.
25. Mackay DJG, Temple IK. Ongoing Challenges in the Diagnosis of 11p15.5-Associated Imprinting Disorders. Mol Diagn Ther. 2022;26(3):263–72. doi:10.1007/s40291-022-00587-1
26. Bliek J, Snijder S, Maas SM, Polstra A, van der Lip K, Alders M, et al. Phenotypic discordance upon paternal or maternal transmission of duplications of the 11p15 imprinted regions. Eur J Med Genet. 2009;52(6):404–8. doi:10.1016/j.ejmg.2009.08.006 PubMed PMID: 19735747.
27. Heide S, Chantot-Bastaraud S, Keren B, Harbison MD, Azzi S, Rossignol S, et al. Chromosomal rearrangements in the 11p15 imprinted region: 17 new 11p15.5 duplications with associated phenotypes and putative functional consequences. J Med Genet. 2018;55(3):205–13. doi:10.1136/jmedgenet-2017-104919 PubMed PMID: 29223973.
28. Begemann M, Spengler S, Gogiel M, Grasshoff U, Bonin M, Betz RC, et al. Clinical significance of copy number variations in the 11p15.5 imprinting control regions: new cases and review of the literature. J Med Genet. 2012;49(9):547–53. doi:10.1136/jmedgenet-2012-100967 PubMed PMID: 22844132; PubMed Central PMCID: PMC3439641.
29. Demars J, Rossignol S, Netchine I, Lee KS, Shmela M, Faivre L, et al. New insights into the pathogenesis of Beckwith-Wiedemann and Silver-Russell syndromes: contribution of small copy number variations to 11p15 imprinting defects. Hum Mutat. 2011;32(10):1171–82. doi:10.1002/humu.21558 PubMed PMID: 21780245.
30. Gabory A, Ripoche MA, Le Digarcher A, Watrin F, Ziyyat A, Forné T, et al. *H19* acts as a trans regulator of the imprinted gene network controlling growth in mice. Development. 2009;136(20):3413–21. doi:10.1242/dev.036061
31. Begemann M, Lengyel A, Pinti E, Kovács ÁF, Fekete G, Stratmann S, et al. Maternal uniparental disomy of chromosome 7: how chromosome 7-encoded imprinted genes contribute to the Silver-Russell phenotype. Clin Epigenetics. 2025;17(1):70. doi:10.1186/s13148-025-01867-3 PubMed PMID: 40307819; PubMed Central PMCID: PMC12042466.
32. Mackay D, Bliek J, Kagami M, Tenorio-Castano J, Pereda A, Brioude F, et al. First step towards a consensus strategy for multi-locus diagnostic testing of imprinting disorders. Clin Epigenetics. 2022;14(1):143. doi:10.1186/s13148-022-01358-9 PubMed PMID: 36345041; PubMed Central PMCID: PMC9641836.
33. Sachwitz J, Strobl-Wildemann G, Fekete G, Ambrozaitytė L, Kučinskas V, Soellner L, et al. Examinations of maternal uniparental disomy and epimutations for chromosomes 6, 14, 16 and 20 in Silver-Russell syndrome-like phenotypes. BMC Med Genet. 2016;17:20. doi:10.1186/s12881-016-0280-8 PubMed PMID: 26969265; PubMed Central PMCID: PMC4787016.
34. Wimmer K, Decker M, Mayatepek E, Beiglböck H, Eggermann T, Kehrer-Sawatzki H, et al. Silver-Russell syndrome-like features in a patient carrying a novel NF1 mutation. Pediatr Res. 2005;58(6):1265–8. doi:10.1203/01.pdr.0000183661.81772.f8 PubMed PMID: 16306205.
35. Zanoni P, Steindl K, Sengupta D, Joset P, Bahr A, Sticht H, et al. Loss-of-function and missense variants in NSD2 cause decreased methylation activity and are associated with a distinct developmental phenotype. Genet Med. 2021;23(8):1474–83. doi:10.1038/s41436-021-01158-1 PubMed PMID: 33941880; PubMed Central PMCID: PMC8354849.
36. Hara-Isono K, Inoue T, Nakamura A, Fuke T, Yamazawa K, Matsubara K, et al. Investigation of methylation profiles in Silver–Russell syndrome to explore episignatures. Clin Epigenet. 2025;17(1):184. doi:10.1186/s13148-025-01993-y
37. Muurinen M, Hannula-Jouppi K, Reinius LE, Söderhäll C, Merid SK, Bergström A, et al. Hypomethylation of HOXA4 promoter is common in Silver-Russell syndrome and growth restriction and associates with stature in healthy children. Sci Rep. 2017;7(1):15693. doi:10.1038/s41598-017-16070-5
38. Prickett AR, Ishida M, Böhm S, Frost JM, Puszyk W, Abu-Amero S, et al. Genome-wide methylation analysis in Silver–Russell syndrome patients. Hum Genet. 2015;134(3):317–32. doi:10.1007/s00439-014-1526-1
39. Wu D, Gong C, Su C. Genome-wide analysis of differential DNA methylation in Silver-Russell syndrome. Sci China Life Sci. 2017;60(7):692–9. doi:10.1007/s11427-017-9079-7
40. Cheng S, Qian F, Huang Q, Wei L, Fu Y, Du Y. HOXA4, down-regulated in lung cancer, inhibits the growth, motility and invasion of lung cancer cells. Cell Death Dis. 2018;9(5):465. doi:10.1038/s41419-018-0497-x

41. Sobreira N, Brucato M, Zhang L, Ladd-Acosta C, Ongaco C, Romm J, et al. Patients with a Kabuki syndrome phenotype demonstrate DNA methylation abnormalities. Eur J Hum Genet. 2017;25(12):1335–44. doi:10.1038/s41431-017-0023-0 PubMed PMID: 29255178; PubMed Central PMCID: PMC5865196.
42. Murray PG, Hanson D, Coulson T, Stevens A, Whatmore A, Poole RL, et al. 3-M syndrome: a growth disorder associated with IGF2 silencing. Endocr Connect. 2013;2(4):225–35. doi:10.1530/EC-13-0065 PubMed PMID: 24148222; PubMed Central PMCID: PMC3847915.
43. Pottie L, Adamo CS, Beyens A, Lütke S, Tapaneeyaphan P, De Clercq A, et al. Bi-allelic premature truncating variants in LTBP1 cause cutis laxa syndrome. Am J Hum Genet. 2021;108(6):1095–114. doi:10.1016/j.ajhg.2021.04.016 PubMed PMID: 33991472; PubMed Central PMCID: PMC8206382.
44. Duque Lasio ML, Kozel BA. Elastin-driven genetic diseases. Matrix Biology. 2018;71–72:144–60. doi:10.1016/j.matbio.2018.02.021
45. Motta M, Fasano G, Gredy S, Brinkmann J, Bonnard AA, Simsek-Kiper PO, et al. SPRED2 loss-of-function causes a recessive Noonan syndrome-like phenotype. Am J Hum Genet. 2021;108(11):2112–29. doi:10.1016/j.ajhg.2021.09.007 PubMed PMID: 34626534; PubMed Central PMCID: PMC8595899.

Figures

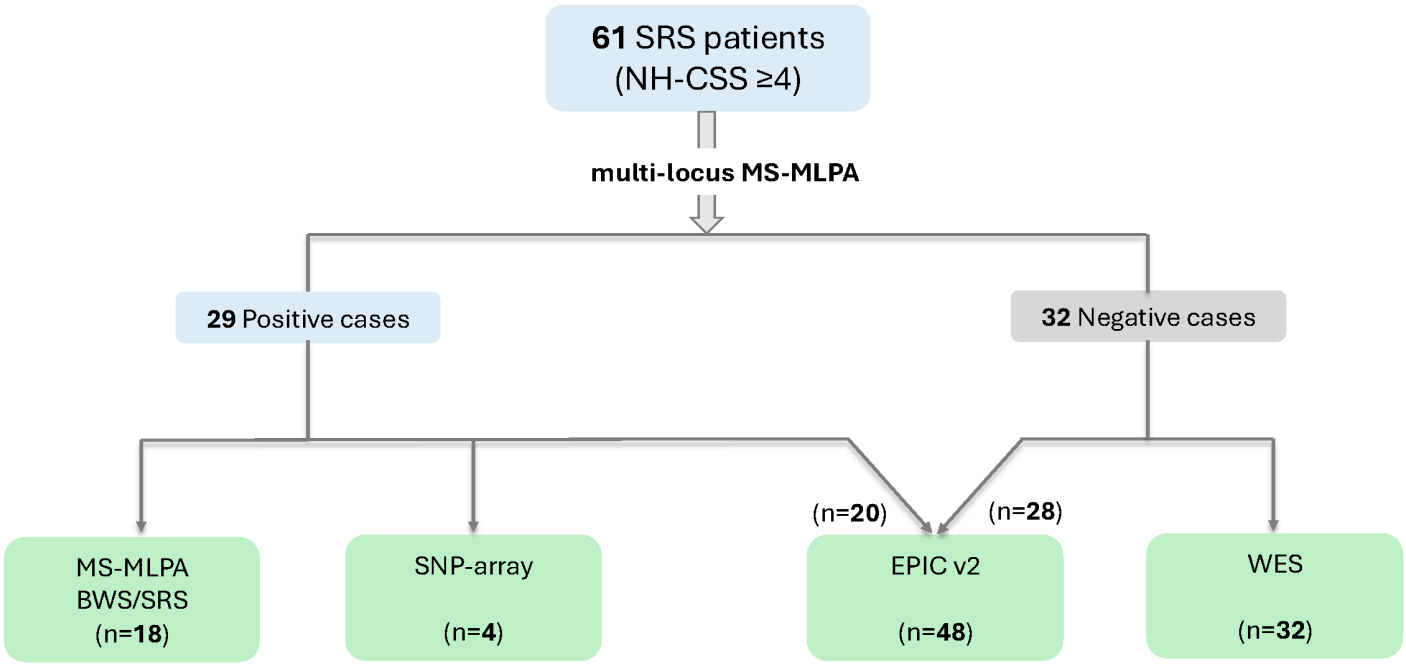


Figure 1

Diagnostic workflow for the molecular characterization of the SRS cohort. A total of 61 patients with suspected SRS met the inclusion criterion of an NH-CSS score ≥4. All patients were first analysed using multi-locus MS-MLPA, which identified molecular defects in 29 cases. Additional analyses were performed using MS-MLPA ME030 and SNP-array. The remaining 32 patients without a molecular diagnosis subsequently underwent whole-exome sequencing. Genome-wide methylation analysis was performed in a subgroup of cases.

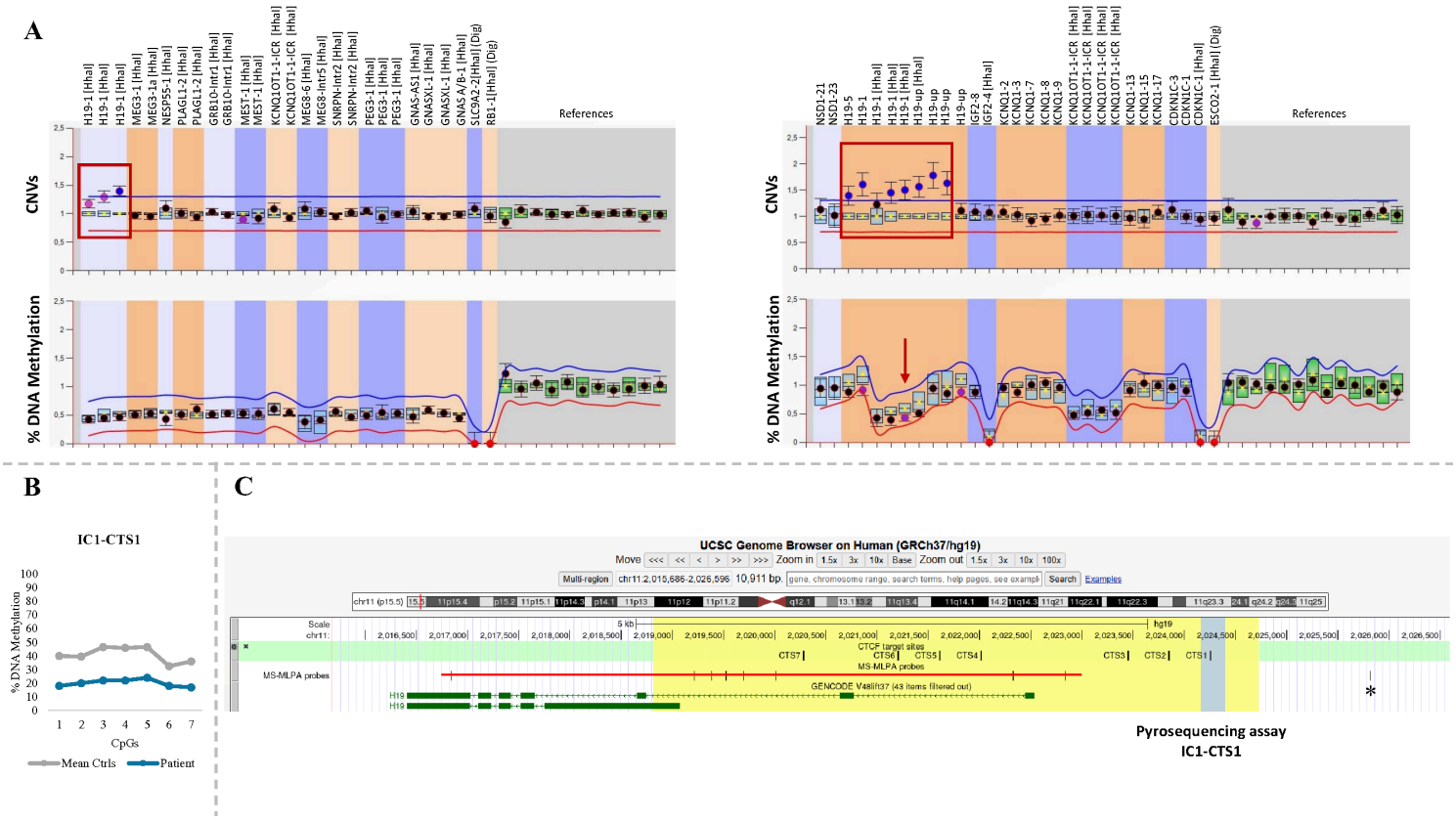


Figure 2

SRS case with *H19* maternal duplication (SRS25). A. Left: Multi-locus MS-MLPA results of case SRS25 showing *H19* duplication. The duplicated probes are indicated by a red rectangle; Right: ME030 MS-MLPA results confirming the *H19* duplication and showing slight hypomethylation at the *H19-IGF2*:IG-DMR. In the upper panel, the duplicated probes are indicated by a red rectangle, whereas in the lower panel the probe showing hypomethylation is indicated by an arrow. **B.** Pyrosequencing results showing methylation levels of CTS1 in the patient and control individuals. **C.** Screenshot from the UCSC Genome Browser (GRCh37/h19) showing the *H19/IGF2*:IG-DMR in yellow. In light blue, the region analysed by pyrosequencing. On the green line, CTCF target sites (CTSs) are shown. Below the CTSs, MS-MLPA probes (kit BWS/SRS) are represented as tiny black lines. The red line indicates the MS-MLPA probes detecting the duplication; the last probe on the right (*) lies outside the duplicated region.



Figure 3

Genome-wide methylation analysis of SRS patients. A. Left: DNA methylation changes at *HOXA4* CpGs covered by EPICv2 for all SRS patients, normalized to controls; Right: DNA methylation changes at *H0XA4*CpGs covered by EPICv2 for the three SRS molecular subgroups, normalized to controls. **B.** Left: DNA methylation changes at *LTBP1* CpGs covered by EPICv2 for SRS patients, normalized to controls; Right: DNA methylation changes at *LTBP1* CpGs covered by EPICv2 for the three SRS molecular subgroups, normalized to controls. **C.** Screenshot from UCSC Genome Browser (GRCh38/hg38) showing that the hypermethylated CpGs overlap with the promoter region of *LTBP1S* isoform.

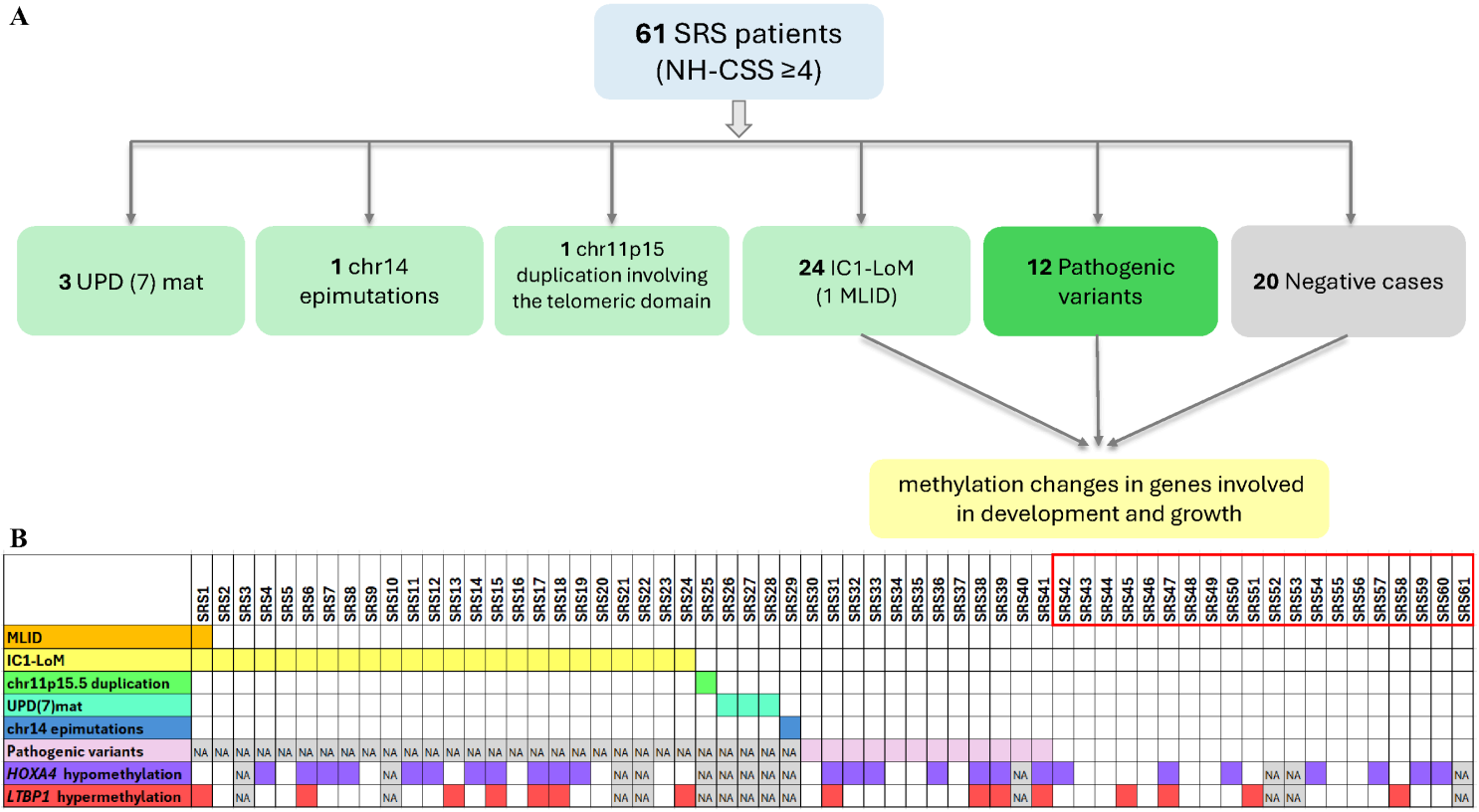


Figure 4

Integrated molecular findings in the Silver-Russell syndrome cohort. A. Schematic summary of molecular results obtained in 61 clinically diagnosed SRS patients (NH-CSS ≥ 4). Molecular defects were identified in 41 patients: three cases with maternal UPD(7), one case with methylation abnormalities on chromosome 14, one patient with a duplication involving the telomeric 11p15 domain, 24 patients with IC1 loss of methylation (including one MLID case), and twelve patients carried pathogenic or likely pathogenic variants in genes associated with growth regulation. 20 cases remained undiagnosed. (light green: defects identified by MS-MLPA/pyrosequencing; green: defects identified by WES; yellow: defects identified by EPICv2) **B.** Integrative representation of molecular alterations identified in individual patients. Each column corresponds to one patient. Coloured boxes indicate the presence of the respective molecular defect. Grey boxes indicate patients for whom WES and/or EPICv2 analyses were not performed. The red rectangle highlights the 20 cases with a negative molecular diagnosis.

Supplementary Files

This is a list of supplementary files associated with this preprint. Click to download.

- Supplementaryfigures.pdf
- Supplementarytables.xlsx